

24. I. Toni, M. Krams, R. Turner, R. Passingham, *Neuroimage* **8**, 50 (1998).
 25. A nonlinear transformation was applied to convert the data from MNI coordinates to those of the Talairach atlas (www.mrc-cbu.cam.ac.uk/Imaging/). Activated regions were identified with both the Talairach atlas (26) and a cerebellum atlas (27).
 26. J. Talairach, P. Tournoux, *Co-Planar Stereotaxic Atlas of the Human Brain. 3-Dimensional Proportional System: An Approach to Cerebral Imaging* (Thieme, New York, 1988) [M. Rayport, Trans.].
 27. J. D. Schmahmann et al., *MRI Atlas of the Human Cerebellum* (Academic Press, San Diego, CA, 2000).
 28. In order to assess expression of learning, sequence block 8 was compared to the average of random blocks 7 and 9, masked with an activation map for the three blocks. Single-participant results were combined in a random effects analysis. An additional random effects analysis was performed to determine

how activation predicted individual performance differences. For this analysis, RT savings at expression, for individual participants, were entered as a regression vector with the expression of learning activation. Thus, the expression contrast searched for areas that showed greater activation during the sequence block than during the two random blocks at expression, and the RT contrast searched for areas that showed greater sequence activation by an amount that was scaled to the individual participants' response time savings. Both contrasts were evaluated at a $P < 0.05$ level. Furthermore, all fMRI data were examined at the group and single-participant level. The results presented at the group level were evident in the analysis of each of the single participants.
 29. J. E. Steinmetz, D. G. Lavond, D. Ivkovich, C. G. Logan, R. F. Thompson, *J. Neurosci.* **12**, 4403 (1992).
 30. R. F. Thompson, D. J. Krupa, *Annu. Rev. Neurosci.* **17**, 519 (1994).

31. R. B. Ivry, S. W. Keele, *J. Cognit. Neurosci.* **1**, 134 (1989).
 32. B. Horwitz, M.-P. Deiber, V. Ibanez, N. Sadato, M. Hallett, *Neuroimage* **12**, 434 (2000).
 33. G. Holmes, *Brain* **63**, 1 (1939).
 34. S. E. Grill, M. Hallett, L. M. McShane, *Exp. Brain Res.* **113**, 33 (1997).
 35. J. Meyer-Lohmann, J. Hore, V. B. Brooks, *J. Neurophysiol.* **40**, 1038 (1977).
 36. T. Tsujimoto, H. Gemba, K. Sasaki, *Brain Res.* **629**, 1 (1993).
 37. We thank R. Shadmehr, S. Wise, T. Ebner, and K. Bushara for comments on the manuscript and H. Shah for assisting in tabulation of the data. This work was supported by NIH grants NS40106 and RR08079, the American Legion Chair in Brain Sciences, and the Department of Veterans' Affairs.
 29 November 2001; accepted 2 April 2002

A Heat-Sensitive TRP Channel Expressed in Keratinocytes

Andrea M. Peier,¹ Alison J. Reeve,² David A. Andersson,²
 Aziz Moqrich,³ Taryn J. Earley,³ Anne C. Hergarden,¹
 Gina M. Story,³ Sian Colley,² John B. Hogenesch,¹
 Peter McIntyre,² Stuart Bevan,² Ardem Patapoutian^{1,3*}

Mechanical and thermal cues stimulate a specialized group of sensory neurons that terminate in the skin. Three members of the transient receptor potential (TRP) family of channels are expressed in subsets of these neurons and are activated at distinct physiological temperatures. Here, we describe the cloning and characterization of a novel thermosensitive TRP channel. TRPV3 has a unique threshold: It is activated at innocuous (warm) temperatures and shows an increased response at noxious temperatures. TRPV3 is specifically expressed in keratinocytes; hence, skin cells are capable of detecting heat via molecules similar to those in heat-sensing neurons.

TRPs belong to a large family of nonselective cation channels that function in a variety of processes, including temperature sensation (1, 2). Vanilloid receptor 1 (TRPV1, also called VR-1) is activated by noxious heat (>42°C) (3). TRPV2 (VRL-1) is also activated by heat, but with a higher threshold (>50°C), whereas TRPM8 (CMR1) is induced by cool/cold temperatures (<25°C) (4–6). A receptor for innocuous warm temperatures has not been identified. Also, the persistent sensitivity of VR-1 knockout animals to moderately noxious heat stimuli implies the presence of another heat receptor (7, 8).

We searched DNA databases for TRPV1-related TRP channels by constructing a hid-

den Markov model (HMM) of the TRPV1 and TRPV2 protein sequences from different mammalian species. With this model, we queried the six-frame translation of human genomic sequences and identified multiple putative exons with a great degree of sequence similarity to the ankyrin and transmembrane domains of TRPV1. We mapped these exons to two genes, one of which is now known as TRPV4 (9, 10). The other gene we have named TRPV3. Full-length sequence of mouse TRPV3 (GenBank accession number AF510316) was derived from a combination of exon prediction software, polymerase chain reaction, and rapid amplification of cDNA ends (RACE) from newborn skin cDNA (11). Several murine expressed sequence tags from skin tissues contain 3'-untranslated region TRPV3 sequence (e.g., BB148735, BB148088), and recently the human TRPV3 sequence has been annotated in GenBank (accession numbers GI 185877 and GI 18587705) (12).

The predicted TRPV3 protein is composed of 791 amino acid residues. The overall

sequence of mouse TRPV3 has 43% identity to TRPV1 and TRPV4, 41% to TRPV2, and 20% to TRPV5 and TRPV6 (fig. S1). TRPV3 has six putative transmembrane domains and four predicted NH₂-terminal ankyrin domains that are thought to be involved in protein-protein interactions. We also identified two coiled-coil domains NH₂-terminal to the ankyrin domains in TRPV3 (fig. S1). Coiled-coil domains have been previously reported to be present in some TRP channels, but not in TRPVs (6, 13). Further examination showed that TRPV1, but not the other members of the TRPV family, also has putative coiled-coil domains in the same location. Interestingly, both TRPV1 and TRPV3 were predicted to reside on human chromosome 17p13 and mouse chromosome 11B4. Our mapping analysis of bacterial artificial chromosome clones, and later the assembled human and mouse genome sequences, revealed the distance between the two genes to be about 10 kb (Fig. 1B) (14).

Given the high degree of homology of TRPV3 to TRPV family members, we tested whether TRPV3 responds to stimuli that activate other closely related family members. The murine full-length TRPV3 was stably expressed in Chinese hamster ovary (CHO) cells, which do not express an endogenous TRPV3 isoform (11, 14). Transfected cells were assayed electrophysiologically by whole-cell voltage-clamp techniques (11). Capsaicin (1 μM), an activator of TRPV1, did not evoke a response in TRPV3-expressing cells (14). Similarly, no current responses were seen when TRPV3-expressing cells were challenged with a hypo-osmotic solution containing 70 mM NaCl or with low pH (pH 5.4) (14). However, raising the temperature of superfused external solution from room temperature to 45°C evoked currents in TRPV3-expressing cells. Analysis of currents evoked by temperature ramps from ~15° to ~48°C (Fig. 2A) showed that little current was elicited until temperatures rose above ~33°C and that the current continued to increase in the noxious temperature range

¹Genomics Institute of the Novartis Research Foundation, San Diego, CA 92121, USA. ²Novartis Institute for Medical Sciences, London WC1E 6BN, UK. ³Department of Cell Biology, Scripps Research Institute, La Jolla, CA 92037, USA.

*To whom correspondence should be addressed. E-mail: ardem@scripps.edu

REPORTS

(>42°C). With these findings, TRPV3-expressing cells were subsequently maintained at 33°C to avoid constitutive activation. The current amplitude was influenced by the presence or absence of Ca²⁺ in the external medium, with reduced current amplitudes in the presence of 2 mM Ca²⁺ after a prior challenge in Ca²⁺-free solution (Fig. 2B). This finding is reminiscent of the channel properties of TRPV5 and TRPV6 (15). The heat-evoked current in TRPV3-expressing CHO cells increased exponentially at temperatures above 35°C, with a factor of *e* (2.71828) increase per 5.29° ± 0.35°C (*n* = 12), corresponding to a mean *Q*₁₀ (increase in reaction rate per 10°C increase in temperature) of 6.62 (Fig. 2C). This temperature dependence is considerably greater than that seen for most ion channel currents, which typically have *Q*₁₀ values in the range 1.5 to 2.0, but is less than the values noted for TRPV1 (*Q*₁₀ = 17.8) (16). In some cells, it was difficult to see a sharp threshold temperature. However, measurable temperature-dependent currents below 30°C showed a factor of *e* increase for a 22.72° ± 3.31°C (*n* = 12) increase in temperature (*Q*₁₀ = 1.69).

The elevated temperature-evoked currents in TRPV3-expressing cells showed a pronounced outward rectification (Fig. 2D) with a reversal potential in the standard recording solution of -1.22 ± 1 mV. Reducing the NaCl in the external solution to 70 mM (from 140 mM) shifted the reversal potential by -19 mV, as expected for a cation-selective conductance (shift = -17.5 mV). Differences in reversal potentials were also used to determine the ionic selectivity of TRPV3 channels. In simplified external solutions, the reversal potentials of the heat-activated currents were similar when NaCl (*E*_{rev} = -1.22 ± 1.08 mV, *n* = 5) was replaced with either KCl (*E*_{rev} = -0.40 ± 0.77 mV, *n* = 6) or CsCl (*E*_{rev} = -1.14 ± 0.53 mV, *n* = 6), which respectively yield relative permeability ratios *P*_K/*P*_{Na} and *P*_{Cs}/*P*_{Na} close to 1. The relative permeabilities of Ca²⁺ and Mg²⁺ were estimated from the shift in reversal potentials when their concentrations were raised from 1 mM to 30 mM in a 100 mM NaCl solution containing the divalent cation under investigation. The reversal potential shifts (from -9.1 ± 1.40 mV to +11.29 ± 0.38 mV for Ca²⁺, and from -8.41 ± 0.50 mV to +10.34 ± 2.38 mV for Mg²⁺) correspond to *P*_{Ca}/*P*_{Na} = 2.57 and *P*_{Mg}/*P*_{Na} = 2.18, respectively. Thus, TRPV3 is a nonselective cation channel that discriminates poorly between the tested monovalent cations and has significant divalent cation permeability.

Heat activation of TRPV3 showed a marked sensitization with repeated heat stimulation. This was studied at a steady membrane potential of -60 mV and with voltage ramps. The first response to a step increase

from room temperature to ~45°C was often very small, but the current response grew with repeated heat steps (Fig. 3A). Sensitization to heat has also been observed for TRPV1 and TRPV2 (4, 17). Application of voltage ramps showed that sensitization was associated with an increase in outward rectification (Fig. 3B). A protocol of repeated temperature challenges was used to investigate whether antagonists of TRPV1 were inhibitors of TRPV3. Under normal conditions, a heat challenge delivered 2 min after four or five sensitizing heat steps evoked a current that was 1.57 ± 0.25 (*n* = 4) times the amplitude of the preceding response (Fig. 3C). Application of 10 μM capsazepine, a competitive capsaicin antagonist at TRPV1, for 2 min before the test heat challenge did

not reduce the current amplitude (2.31 ± 0.36 times the amplitude of the preceding response, *n* = 4). In contrast, a similar exposure to 1 μM ruthenium red, a noncompetitive inhibitor of other TRPV channels, reduced the current to 0.34 ± 0.03 (*n* = 5) times the amplitude of the preceding response (Fig. 3D). Taken together, these results indicate that TRPV3 is a cation-permeable channel activated by warm and hot temperatures and has channel properties reminiscent of other TRPV channels.

To determine the overall expression pattern of the heat-activated TRPV3 channel, we used the full-length mouse TRPV3 sequence as a probe for Northern blot analysis (11). No TRPV3 expression was detected with commercial Northern blots (14). We then used

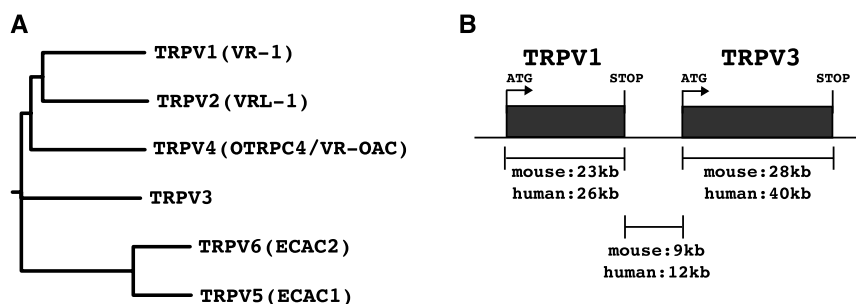


Fig. 1. TRPV3 sequence and genomic localization. (A) Rooted tree showing protein sequence relationship of different members of the TRPV ion channel family. (B) Relative position of TRPV1 and TRPV3 coding sequences on mouse (11B4) and human (17p13) chromosomes.

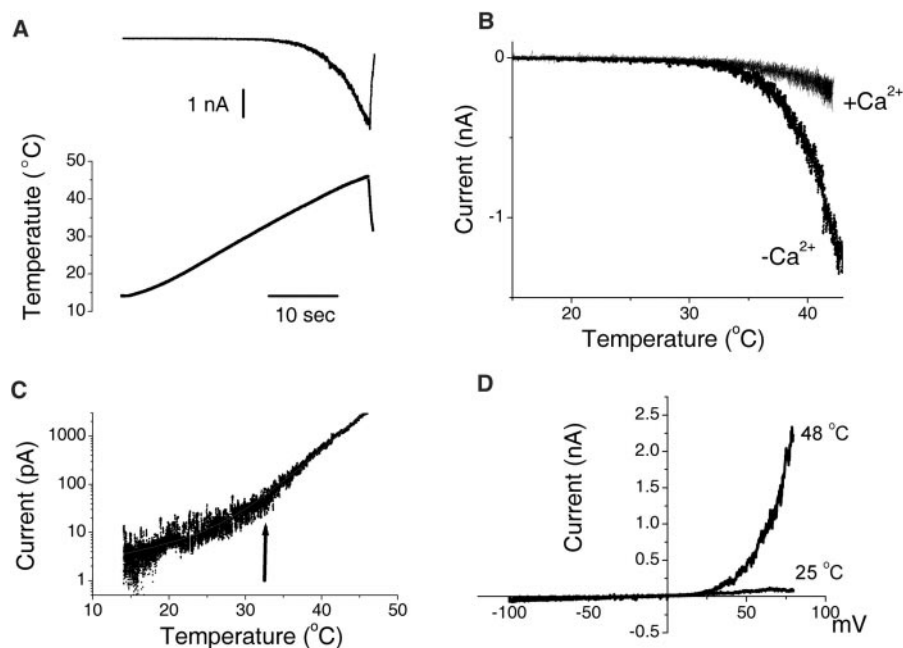


Fig. 2. TRPV3 is activated by heat. Currents were evoked by heat in TRPV3-expressing CHO cells. (A) Inward current to temperature ramp (holding potential *V*_h = -60 mV) in calcium-free external solutions. (B) Heat-evoked currents of the same cell in Ca²⁺-free and subsequently in Ca²⁺-containing solutions showing increased inward current in Ca²⁺ conditions (*V*_h = -60 mV). (C) Semilogarithmic plot of current against temperature with double-exponential fitted line for the same trace as (A). Note the discontinuity at ~33°C (arrow). (D) Current-voltage relation in calcium-containing external solution showing the pronounced outward rectification of TRPV3 at 48°C but not at room temperature. Note the small outward currents at room temperature.

REPORTS

blots from adult rat that included tissues relevant to somatic sensation, including dorsal root ganglia (DRG), spinal cord, and skin (Fig. 4A). An mRNA of ~6.5 kb was present

in tissues derived from skin but not in DRG tissue, although transcripts could be detected in DRG by PCR (14). Probing the same adult blot with a TRPV1-specific probe confirmed

its strong expression in DRG while demonstrating a lack of expression in skin tissues. Northern blot analysis of human adult and fetal skin also showed expression of TRPV3 (14). Cultured primary mouse keratinocytes as well as several epidermal cell lines ($n = 10$) did not show any TRPV3 expression by Northern blots (14). These findings suggest that TRPV3 expression may be down-regulated after tissue dissociation and long-term culture.

Further analysis of TRPV3 expression was performed by ^{35}S radioactive in situ hybridizations on cross sections of newborn mice (11, 18). Clear expression was detected in the epidermis and hair follicles with an antisense probe (Fig. 4B), but not with a control sense probe (14). No expression was detected in DRG (14). To study TRPV3 expression in more detail, we produced polyclonal antibodies to TRPV3 peptides from either the NH_2 -terminus or the COOH -terminus (11). Using either antibody, we observed TRPV3 immunoreactivity in most keratinocytes at the epidermal layer and in hair follicles from newborn and adult rodent tissues (Fig. 4) (14). Coexpression with various keratinocyte-specific markers shows that TRPV3 is expressed in the basal keratinocytes—which in vitro require low calcium concentrations to maintain their undifferentiated state—as well as in some of the more differentiated suprabasal layers of the epidermis (Fig. 4, E to G) (14). Temperature-sensing neurons are thought to terminate as free nerve endings mainly at the level of dermis, but some processes do extend into the epidermis (19, 20). Cutaneous termini can be labeled with the immunohistochemical marker protein gene product 9.5 (PGP 9.5), and we show that these epidermal endings indeed colocalize

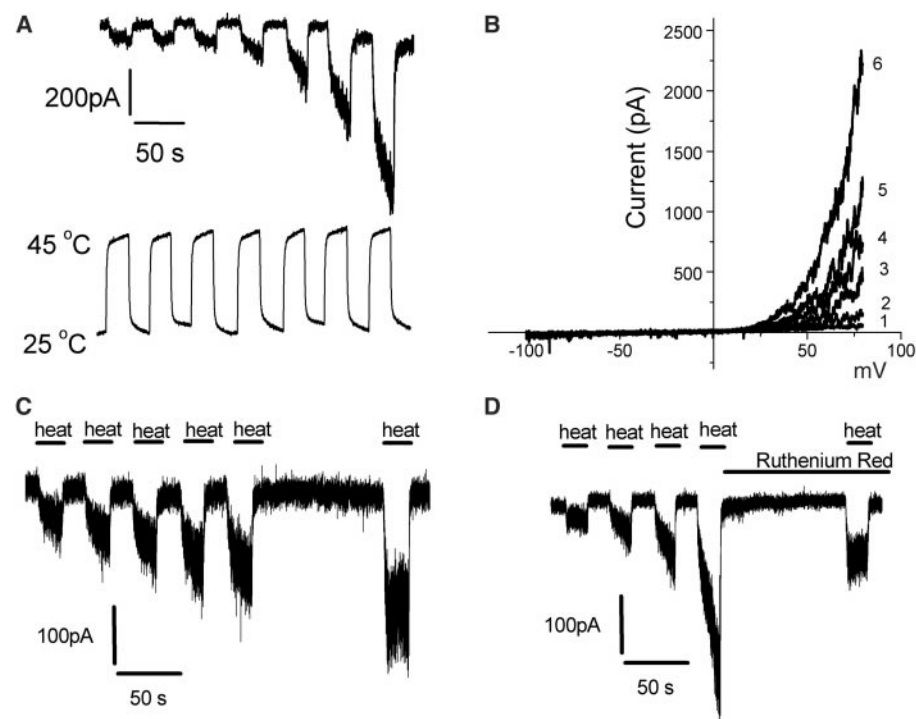
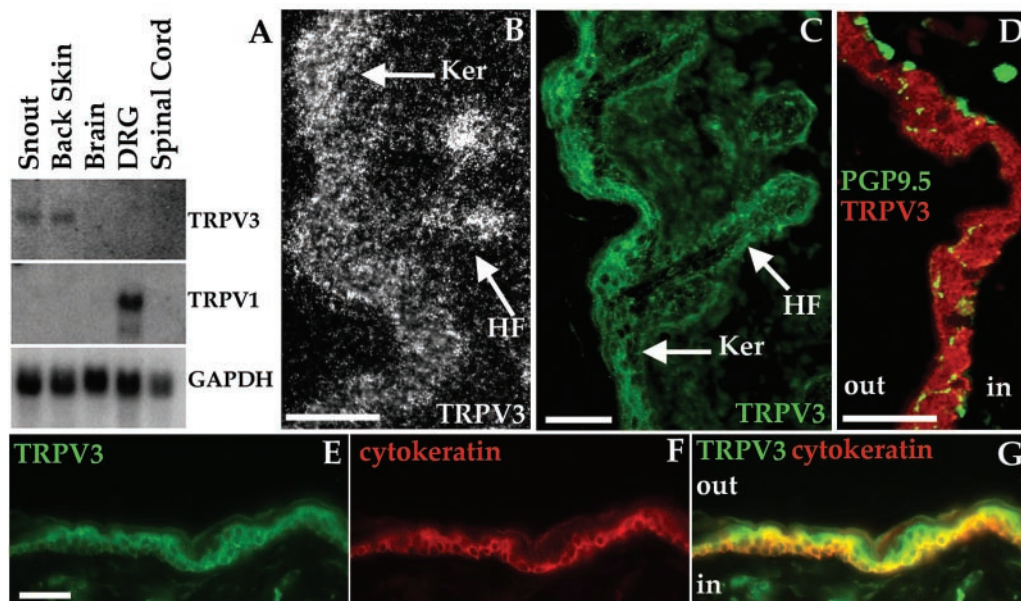


Fig. 3. TRPV3 becomes sensitized to repeated applications of the heat stimulus. (A) Repeated heat steps from 25° to 45°C evoke increased inward current responses ($V_h = -60$ mV). (B) The outward rectification becomes more pronounced with repeated voltage ramps in 48°C external solution. Note that the inward current here showed a only small (factor of <1.5) increase when the temperature was maintained at 48°C, while the outward current increased by a factor of >15. The experiments in (A) and (B) were conducted in the presence of 2 mM CaCl_2 in the external solution. (C) Control protocol for antagonist experiments. Note that the responses continue to sensitize with repeated heat steps in the absence of putative antagonists ($V_h = -60$ mV). (D) Ruthenium red (1 μM) attenuates the sensitization and inhibits the heat response ($V_h = -60$ mV).

Fig. 4. TRPV3 is expressed in keratinocytes. (A) Northern blot analysis of adult rat tissues reveals TRPV3 expression in skin but not in DRG. The blot was hybridized with TRPV3 cDNA, then reprobed with TRPV1 and glyceraldehyde phosphate dehydrogenase (GAPDH) cDNA. (B) In situ hybridization showing expression of TRPV3 in the keratinocytes (Ker) and hair follicle (HF) of newborn mice. (C) Immunostaining for TRPV3 shows similar expression as in (B). (D) TRPV3 and PGP 9.5 immunostaining in adult rat keratinocytes show the presence of free nerve endings at the TRPV3-expressing cell layer. "In" designates the dermal layer. (E to G) TRPV3 and basal pan-cytokeratin immunostaining in adult rat keratinocytes illustrate TRPV3 expression in the basal keratinocytes. Additional expression was observed in cells that had begun to differentiate and thus migrated toward the tissue surface. Scale bars, 50 μm .



with TRPV3-expressing cells (Fig. 4D).

TRPV3 is activated at warm and hot temperatures and is expressed in skin cells (fig. S2). TRPV3 signaling may mediate a cell-autonomous response in keratinocytes upon exposure to heat. It is also possible that the heat-induced TRPV3 signal is transferred to nearby free nerve endings, thereby contributing to conscious sensations of warm and hot. This hypothesis is supported by indirect evidence that skin cells can act as thermal receptors. For instance, although dissociated DRG neurons can be directly activated by heat and cold, warm receptors have only been demonstrated in experiments where skin-nerve connectivity is intact (21, 22). TRPV3 has an activation threshold around 33° to 35°C. The presence of such a warm receptor in skin (with a resting temperature of 34°C) and not DRG neurons (with a resting temperature of 37°C at the cell body) would prevent a warm channel such as TRPV3 from being constitutively active at core 37°C temperatures. The residual heat sensitivity in TRPV1 knockout mice may also involve skin cells: Dissociated DRG neurons from TRPV1-null animals do not respond to moderate noxious stimulus at all, whereas skin-nerve preparations from such animals do respond (7, 8, 23). Collectively, these data suggest that a warmth/heat receptor might be present in the skin, in addition to the heat receptors in DRG.

If keratinocytes indeed act as thermal receptors, how then is the information transferred to neurons? Synapses have not been found between keratinocytes and sensory termini; however, ultrastructural studies have shown that keratinocytes contact, and often surround, DRG nerve fibers through membrane-membrane apposition (19, 20). Therefore, heat-activated TRPV3 signal from keratinocytes could be transduced to DRG neurons through direct signaling. One potential signaling mechanism might involve adenosine triphosphate (ATP). P2X₃, an ATP-gated channel, is present in sensory endings, and analysis of P2X₃ knockout mice show a strong deficit in coding of warm temperatures (24, 25). Furthermore, release of ATP from damaged keratinocytes has been shown to cause action potentials in nociceptors via the P2X receptors (26).

References and Notes

1. D. E. Clapham, L. W. Runnels, C. Strubing, *Nature Rev. Neurosci.* **2**, 387 (2001).
2. C. Montell, L. Birnbaumer, V. Flockerzi, *Cell* **108**, 595 (2002).
3. M. J. Caterina et al., *Nature* **389**, 816 (1997).
4. M. J. Caterina, T. A. Rosen, M. Tominaga, A. J. Brake, D. Julius, *Nature* **398**, 436 (1999).
5. D. D. McKemy, W. M. Neuhauser, D. Julius, *Nature* **416**, 52 (2002).
6. A. M. Peier et al., *Cell* **108**, 705 (2002).
7. M. J. Caterina et al., *Science* **288**, 306 (2000).
8. J. B. Davis et al., *Nature* **405**, 183 (2000).
9. W. Liedtke et al., *Cell* **103**, 525 (2000).

10. R. Strotmann, C. Harteneck, K. Nunnenmacher, G. Schultz, T. D. Plant, *Nature Cell Biol.* **2**, 695 (2000).
11. Materials and Methods are available as supporting material on Science Online.
12. J. B. Peng, E. M. Brown, M. A. Hediger, *Genomics* **76**, 99 (2001).
13. M. Funayama, K. Goto, H. Kondo, *Brain Res. Mol. Brain Res.* **43**, 259 (1996).
14. A. Peier et al., data not shown.
15. B. Nilius et al., *J. Physiol.* **527**, 239 (2000).
16. L. Vyklicky et al., *J. Physiol.* **517**, 181 (1999).
17. S. Jordt, D. Julius, *Cell* **108**, 421 (2002).
18. D. G. Wilkinson, in *Essential Developmental Biology, A Practical Approach*, C. Stern, P. Holland, Eds. (Oxford Univ. Press, New York, 1993), pp. 258–263.
19. M. Hilliges, L. Wang, O. Johansson, *J. Invest. Dermatol.* **104**, 134 (1995).
20. N. Cauna, *J. Anat.* **115**, 277 (1973).
21. H. Hensel, A. Iggo, *Pfluegers Arch.* **329**, 1 (1971).
22. H. Hensel, D. R. Kenshalo, *J. Physiol.* **204**, 99 (1969).
23. C. Roza et al., paper presented at the annual meeting of the Society for Neuroscience, San Diego, CA, October 2001.
24. V. Souslova et al., *Nature* **407**, 1015 (2000).
25. D. A. Cockayne et al., *Nature* **407**, 1011 (2000).
26. S. Cook, E. McCleskey, *Pain* **95**, 41 (2002).
27. We thank E. Gardiner and J. Watson for technical help, and N. Hong, S. Kay, J. Mosbacher, U. Muller, P. Schultz, and C. Song for valuable advice. Supported in part by a grant from Novartis. A.P. is a Basil O'Connor scholar.

Supporting Online Material
www.sciencemag.org/cgi/content/full/1073140/DC1
 Materials and Methods
 Figs. S1 and S2

22 April 2002; accepted 8 May 2002
 Published online 16 May 2002;
 10.1126/science.1073140
 Include this information when citing this paper.

Correlated Bursts of Activity in the Neonatal Hippocampus in Vivo

Xavier Leinekugel,^{1,2,3*†} Rustem Khazipov,^{1,4*} Robert Cannon,¹ Hajime Hirase,² Yehezkel Ben-Ari,¹ György Buzsáki^{2*}

The behavior of immature cortical networks in vivo remains largely unknown. Using multisite extracellular and patch-clamp recordings, we observed recurrent bursts of synchronized neuronal activity lasting 0.5 to 3 seconds that occurred spontaneously in the hippocampus of freely moving and anesthetized rat pups. The influence of slow rhythms (0.33 and 0.1 hertz) and the contribution of both γ -aminobutyric acid A–mediated and glutamate receptor–mediated synaptic signals in the generation of hippocampal bursts was reminiscent of giant depolarizing potentials observed in vitro. This earliest pattern, which diversifies during the second postnatal week, could provide correlated activity for immature neurons and may underlie activity-dependent maturation of the hippocampal network.

Although a variety of oscillatory and intermittent population patterns have been described in the adult central nervous system (1, 2), the expression of neuronal activity in the developing brain remains largely unknown. Previous in vitro investigations in hippocampus and neocortex have revealed a number of major developmentally regulated changes in synaptic transmission properties, including a switch from excitatory to inhibitory effects of γ -aminobutyric acid A (GABA_A) receptor–mediated sig-

nals (3–7), and rapid changes in glutamate receptor expression and synaptic connectivity (7–10). Therefore, the patterns of activity expressed at these early stages of development may be quite different from those expressed in the adult brain.

In the neonatal hippocampus and neocortex, oscillatory patterns have been described in vitro. These include giant depolarizing potentials (GDPs) (3, 5, 7, 11–14) in the hippocampus, cortical early network oscillations [cENOs (15)], and synchronized domains (16–19) in the neocortex. However, the activities expressed in vivo remain unknown. Correlated patterns of activity, either endogenously generated or initiated by sensory inputs, may be a general requirement for the proper development of central nervous structures (7, 14, 20–22). Because the early postnatal period is critical for the activity-dependent maturation of synaptic connections in the cortical structures of the rat (20–23), it is important to reveal the physiological patterns expressed in these structures in vivo.

¹INMED, Institut National de la Santé et de la Recherche Médicale (INSERM) U29, Avenue de Luminy, Boite Postale 13, 13273 Marseille Cedex 09, France. ²Center for Molecular and Behavioral Neuroscience, Rutgers University, 197 University Avenue, Newark, NJ 07102, USA. ³INSERM EMI 0224 “Cortex et Epilepsie,” Faculté de Médecine Pitié-Salpêtrière, Université Paris 6, 105 Boulevard de l’Hôpital, 75013 Paris, France. ⁴Children’s Hospital, Harvard Medical School, 300 Longwood Avenue, Boston, MA 02115, USA.

*These authors contributed equally to this work.
 †To whom correspondence should be addressed. E-mail: xlk@noos.fr